HANSER

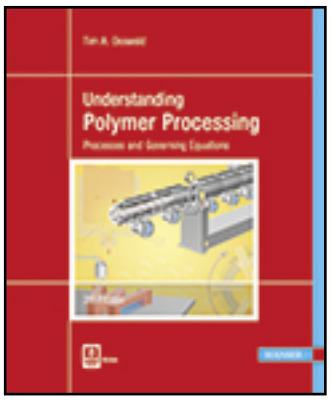

Sample Pages

Tim A. Osswald

Understanding Polymer Processing

Processes and Governing Equations

Book ISBN: 978-1-56990-647-7

eBook ISBN: 978-1-56990-648-4

For further information and order see

www.hanserpublications.com (in the Americas)

www.hanser-fachbuch.de (outside the Americas)

Preface to the Second Edition

This book evolved from Hanser Publishers' textbook *Polymer Processing Fundamentals*, which was revised under the title *Understanding Polymer Processing*. It has now been almost twenty years since the first book appeared, and six years since the latter was published. The last edition of this book has been adopted by several universities in North and South America, Europe, Asia, and Africa as a textbook to introduce engineering students to polymer processing. The changes and additions that were introduced in this edition are based on suggestions from these professors and their students, my own teaching experience, and suggestions from my students, as well as changes that have occurred in the industry in the past few years. Perhaps the biggest addition is an additional chapter on additive manufacturing.

With this edition, the author owes his gratitude to Dr. Mark Smith of Hanser Publishers for editing the book and catching problems and inconsistencies throughout, and Jörg Strohbach for all his assistance with typesetting and template issues. I am grateful to Tobias Mattner for his superb job at re-drawing all the figures and for his suggestions on how to make many of the figures more understandable. A special thanks to Dr. Dominik Rietzel and Martin Friedrich for co-authoring Chapter 7, Additive Manufacturing. Their experience and input on the entire additive manufacturing field and technology was very valuable. Thank you Diane for – as always – serving as a sounding board and advisor during this project, Palitos for your interest in this field, and Rudi for changing things up a bit.

Summer 2017

Tim A. Osswald

Preface to the First Edition

This book provides the background for an understanding of the wide field of polymer processing. It is divided into three parts to give the engineer or student sufficient knowledge of polymer materials, polymer processing and modeling. The book is intended for the person who is entering the plastics manufacturing industry, as well as a textbook for students taking an introductory course in polymer processing.

Understanding Polymer Processing is based on the 12-year-old Hanser Publishers book *Polymer Processing Fundamentals*, as well as lecture notes from a 7-week polymer processing course taught at the University of Wisconsin-Madison.

The first three chapters of this book cover essential information required for the understanding of polymeric materials, from their molecule to their mechanical and rheological behavior. The next four chapters cover the major polymer processes, such as extrusion, mixing, injection molding, thermoforming, compression molding, rotomolding, and more. Here, the underlying physics of each process is presented without complicating the reading with complex equations and concepts, however, helping the reader understand the basic plastics manufacturing processes. The last two chapters present sufficient background to enable the reader to carry out process scaling and to solve back-of-the-envelope polymer processing models.

I cannot possibly acknowledge everyone who helped in the preparation of this manuscript. First, I would like to thank all the students in my polymer processing course who, in the past two decades, have endured my experimenting with new ideas. I am also grateful to my polymer processing colleagues who taught the introductory polymer processing course before me: Ronald L. Daggett, Lew Erwin, Jay Samuels and Jeroen Rietveld. I thank Nicole Brostowitz for adding color to some of the original graphs, and to Katerina Sánchez for introducing and organizing the equations and for proofreading the final manuscript. I would like to thank Professor Juan Pablo Hernández-Ortiz, of the Universidad Nacional de Colombia, Medellín, for his input in Part III of this book. Special thanks to Wolfgang Cohnen for allowing me to use his photograph of Coyote Buttes used to exemplify the Deborah number in Chapter 3. My gratitude to Dr. Christine Strohm, my editor at Hanser Publishers, for her encouragement, support and patience. Thanks to Steffen Jörg at Hanser Publishers for his help and for putting together the final manuscript. Above all, I thank

my wife Diane and my children Palitos and Rudi for their continuous interest in my work, their input and patience.

Summer of 2010

Tim A. Osswald

Contents

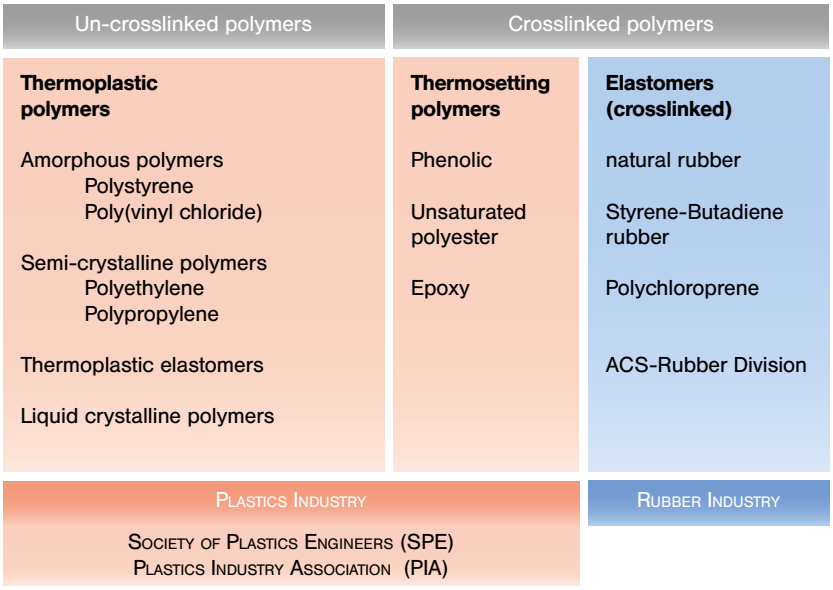

Single screw Extruder

Twin screw Extruder

Injection molding Machine

Special injection molding processes

Figure 1.19 The plastics and rubber industries

More importantly, each industry utilizes its own sets of standards to evaluate the materials. Furthermore, whole companies concentrate on either one or the other industry.

1.10 Polymer Processes

The two main plastics processing techniques are the *extrusion* and *injection molding processes*. As covered in detail in Chapters 4 and 6, the fundamental element of both these manufacturing methods is the screw and heated barrel system, as depicted in Figure 1.20.

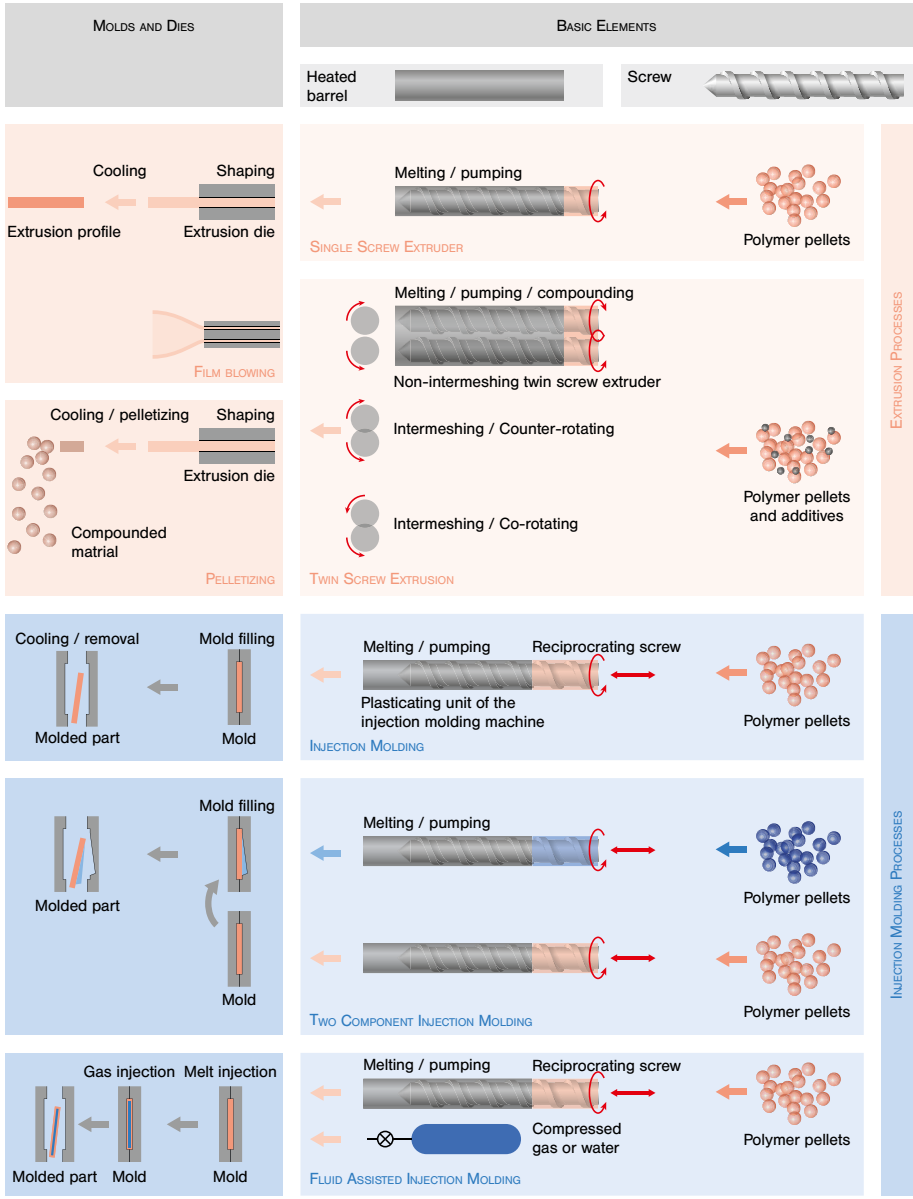

Figure 1.20 Plastics processing break down

The right column in the figure first presents extrusion, with its two major categories, the *single screw extruder* and the *twin screw extruder*. The twin screw system is an arrangement of two screws inside a double or twin barrel, primarily used for mixing (*compounding*). Mixing and compounding is covered in Chapter 5 of this book. Both, the single and twin screw systems, are used for melting the resin, as well as for pumping the polymer melt through the extrusion die. The pumping action is accomplished by generating the pressure required to push the melt through

the die. The die in the extrusion systems are used to shape the material into a continuous product, such as a film, a plate, a tube, a strand, or any desired profile. In most cases, twin screw extruder dies produce strands that are cut into pellets of the compounded plastic or *resin*, which is used in subsequent extrusion or injection molding processes. The pellets that result from a twin screw compounding process are typically pellets of *polymer blends*.

Injection molding is perhaps the most widely and versatile process in the plastics industry. Figure 1.20 presents the process with some of its variations, such as *two-component injection molding*, where one plastic is over-molded on a pre-injected substrate. Related to the two-component injection process is the *co-injection molding process*, where one resin displaces another creating a product with a skin made up of the first resin, and a central core of the second material. If the second material is a fluid, such as nitrogen or water, one creates a hollow part. This type of process can be referred to as *fluid assisted injection molding*. The two commercial fluid assisted processes are the *gas-assisted injection molding* and the *water assisted injection molding processes*.

Problems

1. Estimate the degrees of polymerization of a polyethylene with an average molecular weight between 150,000 and 200,000.
2. What is the maximum possible separation between the ends of a polystyrene molecule with a molecular weight of 160,000?
3. Write the molecular structure for the following polymers: polyacetal, polycarbonate, polyvinyl chloride, polystyrene, and polytetrafluoroethylene.

References

1. Osswald, T.A., and G. Menges, *Materials Science of Polymers for Engineers*, 3rd Ed., Hanser Publishers (2012), Munich
2. de la Condamine, C.M., *Relation Abregee D'un Voyage Fait Dans l'interieur de l'Amerique Meridionale*, Academie des Sciences (1745), Paris
3. DuBois, J.H., *Plastics History U.S.A.*, Cahners Publishing Co., Inc. (1972), Boston
4. Tadmor, Z., and C.G. Gogos, *Principles of Polymer Processing*, John Wiley & Sons (2006), New York
5. McPherson, A.T., and A. Klemin, *Engineering Uses of Rubber*, Reinhold Publishing Corporation (1956), New York
6. Sonntag, R., *Kunststoffe* (1985), *75*, 4
7. Herrmann, H., *Kunststoffe* (1985), *75*, 2
8. Regnault, H.V., *Liebigs Ann.* (1835), *14*, 22
9. Ulrich, H., *Introduction to Industrial Polymers*, 2nd Ed., Hanser Publishers (1993), Munich
10. Rauwendaal, C., *Polymer Extrusion*, 5th Ed., Hanser Publishers (2014), Munich
11. Osswald, T.A., E. Baur, S. Brinkmann, K. Oberbach, and E. Schmachtenberg, *International Plastics Handbook*, Hanser Publishers (2006), Munich
12. Campo, E.A., *Industrial Polymers*, Hanser Publishers (2008), Munich

test results remains the same, except for a horizontal shift to the left or right, representing lower or higher response times, respectively.

2.1.2 Time-Temperature Superposition

The time-temperature equivalence seen in stress relaxation test results can be used to reduce data at various temperatures to one general *master curve* for a reference temperature, *T*. To generate a master curve at any reference temperature, the curves shown on the left of Figure 2.1 must be shifted horizontally, holding the reference curve fixed. The master curve for the data in Figure 2.1 is on the right of the figure. Each curve was shifted horizontally until the ends of all the curves superposed. The amount that each curve was shifted can be plotted with respect to the temperature difference taken from the reference temperature. For the data in Figure 2.1, the shift factor is shown in Figure 2.2. It is important to point out here that the relaxation master curve represents a material at a single temperature, but depending on the time scale, it can be regarded as a Hookean solid, or a viscous fluid. In other words, if the material is loaded for a short time, the molecules are not allowed to move and slide past each other, resulting in a perfectly elastic material. In such a case, the deformation is fully recovered. However, if the test specimen is maintained deformed for an extended period of time, such as 100 hours for the 25 °C case, the molecules will have enough time to slide and move past each other, fully relaxing the initial stresses, resulting in permanent deformation. For such a time scale the material can be regarded as a fluid.

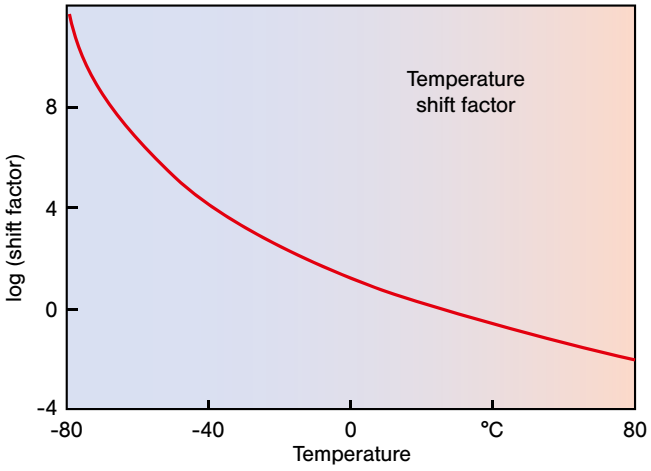

Figure 2.2 Shift factor as a function of temperature used to generate the master curve plotted in Figure 2.1

WLF Equation [2]

The amount relaxation curves must be shifted in the time axis to line-up with the master curve at a reference temperature is represented by

$$\log t - \log t_{ref} = \log\left(\frac{t}{t_{ref}}\right) = \log a_T \tag{2.2}$$

Although the results in Figure 2.2 were shifted to a reference temperature of 298 K (25 °C), Williams, Landel, and Ferry [2] chose T_{ref} = 243 K for

Williams-Landel-Ferry (WLF) equation

$$\log a_T = \frac{-8.86\left(T - T_{ref}\right)}{101.6 + T - T_{ref}} \tag{2.3}$$

which holds for nearly all amorphous polymers if the chosen reference temperature is 45 K above the glass transition temperature. In general, the horizontal shift, $\log a_T$, between the relaxation responses at various temperatures to a reference temperature can be computed using the well known Williams-Landel-Ferry [2] (WLF) equation. The WLF equation is

$$\log a_T = \frac{-C_1\left(T - T_{ref}\right)}{C_2 + T - T_{ref}} \tag{2.4}$$

where C_1 and C_2 are material dependent constants. It has been shown that with $C_1 = 17.44$ and $C_2 = 51.6$, Eq. (2.4) fits well for a wide variety of polymers as long as the glass transition temperature is chosen as the reference temperature. These values for C_1 and C_2 are often referred to as universal constants. Often, the WLF equation must be adjusted until it fits the experimental data. Master curves of stress relaxation tests are important because the polymer's behavior can be traced over much longer periods than those that can be determined experimentally.

Boltzmann Superposition Principle

In addition to the *time-temperature superposition principle* (WLF), the *Boltzmann superposition principle* is of extreme importance in the theory of linear viscoelasticity. The Boltzmann superposition principle states that the deformation of a polymer component is the sum or superposition of all strains that result from various loads acting on the part at different times. This means that the response of a material to a specific load is independent of pre-existing loads. Hence, we can compute the deformation of a polymer specimen upon which several loads act at different points in time by simply adding all strain responses.

2.2 The Short-Term Tensile Test

The most commonly used mechanical test is the short-term stress-strain tensile test. Stress-strain curves for selected polymers are displayed in Figure 2.3 [3]. For comparison, the figure also presents stress-strain curves for copper and steel. Although they have much lower tensile strengths, many engineering polymers exhibit much higher strains at break than metals.

Comparing stress-strain behavior

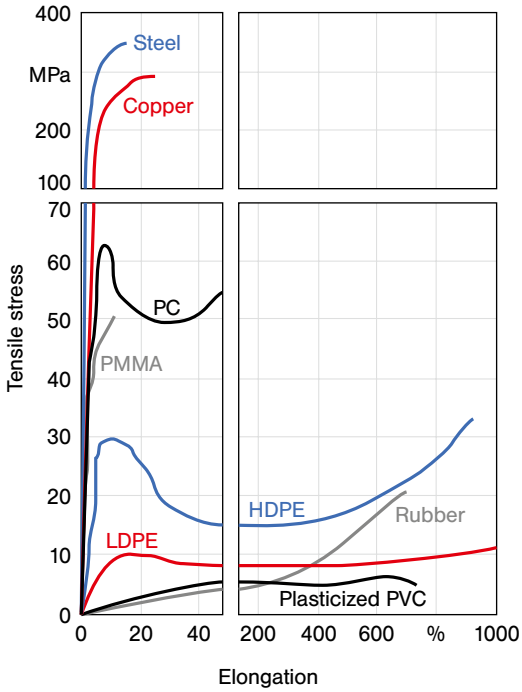

Figure 2.3 Tensile stress-strain curves for several materials

The next two sections discuss the short-term tensile test for cross-linked elastomers and thermoplastic polymers separately. The main reason for separating these two polymers is that the deformation of a crosslinked elastomer and an uncrosslinked thermoplastic differ greatly. The deformation in a crosslinked polymer is generally reversible, while the deformation in typical uncross-linked polymers is associated with molecular chain relaxation, making the process time-dependent and irreversible.

2.2.1 Elastomers

Rubber elasticity

The main feature of cross-linked elastomeric materials is that they can undergo large, reversible deformations. This is because the curled polymer chains stretch

The melt flow indexer can be used for material quality control

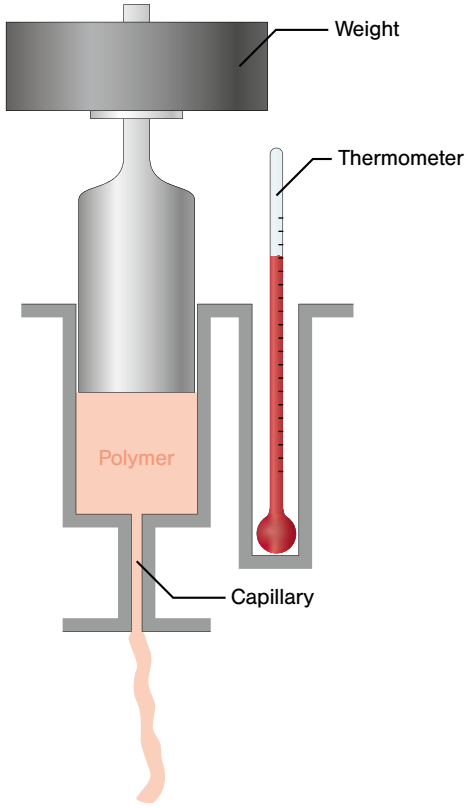

Figure 3.12 Schematic diagram of an extrusion plastometer used to measure melt flow index

3.2.2 The Capillary Viscometer

The most common and simplest device for measuring viscosity is the capillary viscometer. Its main component is a straight tube or capillary, and it was first used to measure the viscosity of water by Hagen [22] and Poiseuille [23]. A capillary rheometer has a pressure driven flow for which the shear rate is maximum at the wall and zero at the center of the flow, making it a non-homogeneous flow [24].

Since pressure driven viscometers employ heterogeneous flows, they can only measure steady shear functions such as viscosity, $\eta(\dot{\gamma})$. However, they are widely used because they are relatively inexpensive and simple to operate. Despite their simplicity, long capillary viscometers provide the most accurate viscosity data available. Another major advantage is that the capillary rheometer has no free surfaces in the test region, unlike other types of rheometers, such as the cone and plate rheometer discussed next. When the strain rate dependent viscosity of polymer melts is measured, capillary rheometers are capable of obtaining such data at shear

rates greater than $10\,s^{-1}$. This is important for processes with higher rates of deformation such as mixing, extrusion, and injection molding. Because its design is basic and it only needs a pressure head at its entrance, the capillary rheometer can easily attach to the end of a screw- or ram-type extruder for online measurements. This makes the capillary viscometer an efficient tool for industry. The basic features of the capillary rheometer are shown in Figure 3.13.

The capillary viscometer can be used to measure viscosity as a function of rate of deformation and temperature

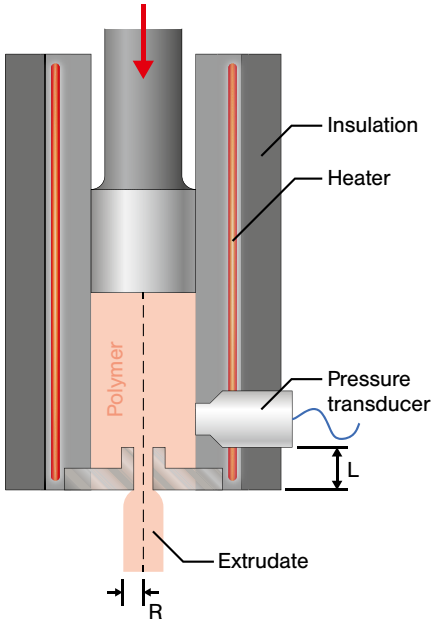

Figure 3.13 Schematic diagram of a capillary rheometer

A capillary tube of radius R and length L is connected to the bottom of a reservoir. Pressure drop and flow rate through this tube are used to determine the viscosity. At the wall, the shear stress is:

$$\tau_w = \frac{R\left(p_0 - p_L\right)}{2L} = \frac{R\Delta p}{2L} \tag{3.11}$$

Equation (3.11) requires that the capillary be long enough to assure fully developed flow, where end effects are insignificant. However, because of entrance effects, the actual pressure profile along the length of the capillary exhibits curvature. The effect is shown schematically in Figure 3.14 [24] and was corrected by Bagley [25] using the end correction e:

$$\tau_w = \frac{R\left(p_0 - p_L\right)}{2(L/D + e)} \tag{3.12}$$

The correction e at a specific shear rate can be found by plotting pressure drop for various capillary L/D ratios, as shown in Figure 3.15.

The cone-and-plate rheometer can be used to measure viscosity as well as first normal stress difference

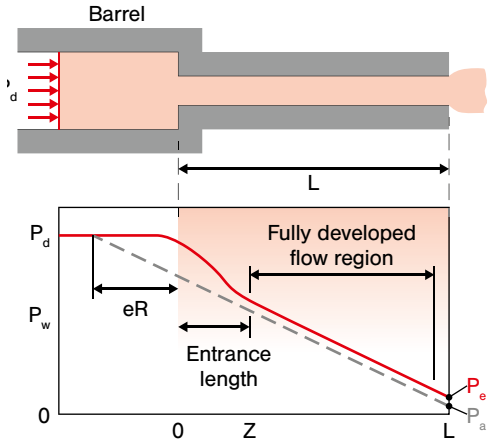

Figure 3.14 Entrance effects in a typical capillary viscometer

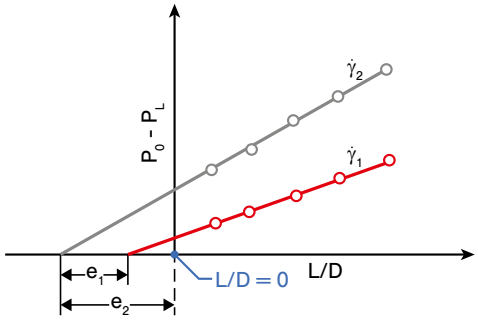

Figure 3.15 Bagley plots for two shear rates

The equation for shear stress is then

$$\tau_{rz} = \frac{r}{R}\tau_w \tag{3.13}$$

To obtain the shear rate at the wall the Weissenberg-Rabinowitsch [26] equation can be used

$$\dot{\gamma}_w = \frac{1}{4}\dot{\gamma}_{aw}\left(3 + \frac{d(\ln Q)}{d(\ln \tau)}\right) \tag{3.14}$$

where, $\dot{\gamma}_{aw}$ is the apparent or Newtonian shear rate at the wall and is written as

$$\dot{\gamma}_{aw} = \frac{4Q}{\pi R^3} \tag{3.15}$$

The shear rate and shear stress at the wall are now known. Therefore, using the measured values of the flow rate, Q, and the pressure drop, $p_0 - p_L$, the viscosity is calculated using

$$\eta = \frac{\tau_w}{\dot{\gamma}_w} \tag{3.16}$$

3.2.3 The Cone-and-Plate Rheometer

The cone-and-plate rheometer is another rheological measuring device widely accepted in the polymer industry. Here, a disc of polymer is squeezed between a plate and a cone, as shown in Figure 3.16. When the disc is rotated, the torque and the rotational speed are related to the viscosity and the force required to keep the cone at the plate is related to the first normal stress difference. The secondary normal stress difference is related to the pressure distribution along the radius of the plate.

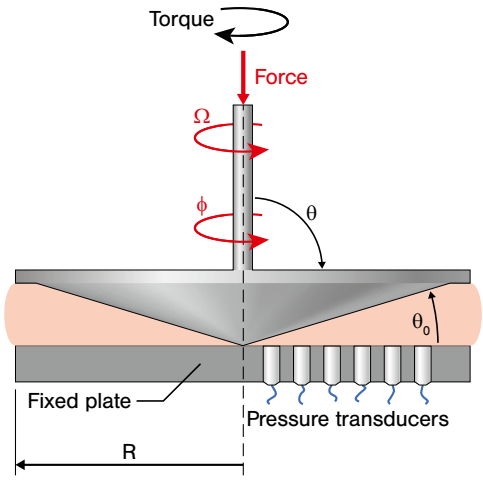

Figure 3.16 Schematic diagram of a cone-plate rheometer

Problems

1. Estimate the consistency index, m, and the power-law index, n, for the ABS at 220 °C presented in Figure 3.2.
2. Estimate the consistency index, m, and the power-law index, n, for the PC at 340 °C presented in Figure 3.2.
3. Use Eq. (3.3) to fit the consistency index for the PC presented in Figure 3.2.
4. You are to extrude a polystyrene sheet through a die with a land length of 0.1 meters. What is the maximum speed you can extrude the sheet if the relaxation time of the polystyrene is 0.5 seconds for the given processing temperature?

5. Estimate the consistency index of the ABS at 220 °C after adding 20 % by volume of micro glass beads.
6. How important is the elastic response inside an internal batch mixer when the rotors turn at 60 rpm, if the relaxation time of the rubber compound is 5 seconds?

References

[1] Giacomin, A.J., T. Samurkas, and J.M. Dealy, *Polym. Eng. Sci.* (1989), *29*, 499

[2] Ostwald, W., *Kolloid-Z.* (1925), *36*, 99

[3] de Waale, A., *J. Oil Colour Chem. Assoc.* (1923), *6*, 33

[4] Laun, H.M., *Rheol. Acta* (1978), *17*, 1

[5] Tadmor, Z., and R.B. Bird, *Polym. Eng. Sci.* (1974), *14*, 124

[6] Agassant, J.-F., Avenas, P., Carreau, P.J., Vergnes, B., Vincent, M., *Polymer Processing: Principles and Modeling*, 2nd Ed., Hanser Publishers (2017), Munich

[7] Vinogradov, G.V., A.Y., Malkin, Y.G. Yanovskii, E.K. Borisenkova, B.V. Yarlykov, and G.V. Berezhnaya, *J. Polym. Sci. Part A-2* (1972), *10*, 1061

[8] Vlachopoulos, J., and M. Alam, *Polym. Eng. Sci.* (1972), *12*, 184

[9] Osswald, T.A., and G. Menges, *Materials Science of Polymers for Engineers*, 3rd Ed., Hanser Publishers (2012), Munich

[10] Spencer, R.S., and R.D. Dillon, *J. Colloid Interface Sci.* (1947), *3*, 163

[11] Denn, M.M., *Annu. Rev. Fluid Mech.* (1990), *22*, 13

[12] Castro, J.M., and C.W. Macosko, *AIChe J.* (1982), *28*, 250

[13] Castro, J.M., S.J. Perry, and C.W. Macosko, *Polym. Commun.* (1984), *25*, 82

[14] Guth, E., and R. Simha, *Kolloid-Z.* (1936), 74, 266

[15] Keunings, R., *Simulation of Viscoelastic Fluid Flow*, in *Computer Modeling for Polymer Processing*, C.L. Tucker, III (Ed.), Hanser Publishers (1989), Munich

[16] Crochet, M.J., A.R. Davies, and K. Walters, *Numerical Simulation of Non-Newtonian Flow*, Elsevier (1984), Amsterdam

[17] Debbaut, B., J.M. Marchal, and M.J. Crochet, *J. Non-Newtonian Fluid Mech.* (1988), *29*, 119

[18] Dietsche, L., and J. Dooley, *SPE ANTEC* (1995), *53*, 188

[19] Dooley, J., and K. Hughes, *SPE ANTEC* (1995), *53*, 69

[20] Baaijens, J.P.W., *Evaluation of Constitutive Equations for Polymer Melts and Solutions in Complex Flows*, Ph.D. Thesis (1994), Eindhoven University of Technology, Eindhoven, The Netherlands

[21] ASTM, 8.01, Plastics (I), ASTM (1994), Philadelphia

[22] Hagen, G.H.L., *Ann. Phys.* (1839), *46*, 423

[23] Poiseuille, L.J., *C. R. Hebd. Seances Acad. Sci.* (1840), *11*, 961

[24] Dealy, J.M., *Rheometers for Molten Plastics*, Van Nostrand Reinhold Company (1982), New York

[25] Bagley, E.B., *J. Appl. Phys.* (1957), *28*, 624

[26] Rabinowitsch, B., *Z. Phys. Chem.* (1929), *145*, 1

[27] Osswald, T.A., and Rudolph, N., *Polymer Rheology – Fundamentals and Applications*, Hanser Publishers (2014), Munich

6.3.4 Injection-Compression Molding

CD's are injection Compression molded to reduce molecular orientation and cycle time

The injection-compression molding (ICM) is an extension of conventional injection molding by incorporating a mold compression action to compact the polymer material for producing parts with dimensional stability and surface accuracy. In this process, the mold cavity has an enlarged cross-section initially, which allows polymer melt to proceed readily to the extremities of the cavity under relatively low pressure. At some time during or after filling, the mold cavity thickness is reduced by a mold-closing movement, which forces the melt to fill and pack out the entire cavity. This mold compression action results in a more uniform pressure distribution across the cavity, leading to more homogeneous physical properties and less shrinkage, warpage, and molded-in stresses than are possible with conventional injection molding. The injection-compression molding process is schematically depicted in Figure 6.22. A potential drawback associated with the two-stage sequential ICM is the *hesitation* or *witness* mark resulting from flow stagnation during injection-compression transition. To avoid this surface defect and to facilitate continuous flow of the polymer melt, *simultaneous ICM* activates mold compression while resin is being injected. The primary advantage of ICM is the ability to produce dimensionally stable, relatively stress-free parts, at a low pressure, clamp tonnage (typically 20 to 50% lower than with injection molding), and reduced cycle time. For thin-wall applications, difficult-to-flow materials, such as polycarbonate, have been molded as thin as 0.5 mm. Additionally, the compression of a relatively circular charge significantly lowers molecular orientation, consequently leading to reduced birefringence, improving the optical properties of a finished part. ICM is the most suitable technology for the production of high-quality and cost-effective CD-audio/ROMs as well as many types of optical lenses.

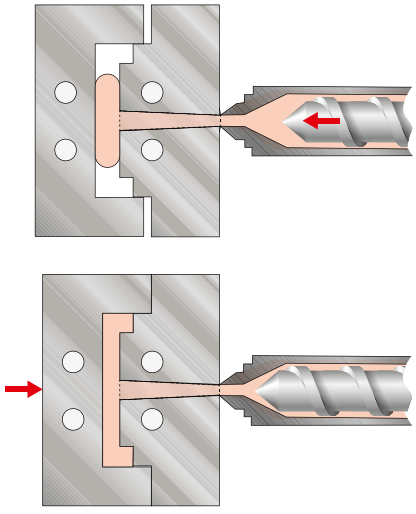

Figure 6.22 Schematic of the injection-compression molding process

6.3.5 Reaction Injection Molding (RIM)

Reaction injection molding (RIM) involves mixing of two reacting liquids in a mixing head before injecting the low-viscosity mixture into mold cavities at relatively high injection speeds. The liquids react in the mold to form a cross-linked solid part. Figure 6.23 presents a schematic of a high pressure polyurethane injection system. The mixing of the two components occurs at high speeds in *impingement mixing heads*. Low pressure polyurethane systems, such as the one schematically presented in Figure 6.24, require mixing heads with a mechanical stirring device. The short cycle times, low injection pressures, and clamping forces, coupled with superior part strength and heat and chemical resistance of the molded part make RIM well suited for the rapid production of large, complex parts, such as automotive bumper covers and body panels. Reaction injection molding is a process for rapid production of complex parts directly from monomers or oligomers. Unlike thermoplastic injection molding, the shaping of solid RIM parts occurs through polymerization (cross-linking or phase separation) in the mold rather than solidification of the polymer melts. RIM is also different from thermoset injection molding in that the polymerization in RIM is activated via chemical mixing rather than thermally activated by the warm mold. During the RIM process, the two liquid reactants (e.g., polyol and an isocyanate, which were the precursors for polyurethanes) are metered in the correct proportion into a mixing chamber where the streams impinge at a high velocity and start to polymerize prior to being injected into the mold. Due to the low-viscosity of the reactants, the injection pressures are typically very low, even though the injection speed is fairly high. Because of the fast reaction rate, the final parts can be de-molded in typically less than one minute. There are a number of RIM variants. For example, in the so-called reinforced reaction injection molding (RRIM) process, fillers, such as short glass fibers or glass flakes, have been used to enhance the stiffness, maintain dimensional stability, and reduce material cost of the part. As another modification of RIM, structural reaction injection molding (SRIM) is used to produce composite parts by impregnating a reinforcing glass fiber-mat (preform) preplaced inside the mold with the curing resin. Resin transfer molding (RTM) is very similar to SRIM in that it also employs reinforcing glass fiber-mats to produce composite parts; however, the resins used in RTM are formulated to react more slowly, and the reaction is thermally activated as it is in thermoset injection molding. The capital investment for molding equipment for RIM is lower compared with that for injection molding machines. Finally, RIM parts generally exhibit greater mechanical and heat-resistant properties due to the resulting cross-linking structure. The mold and process designs for RIM become generally more complex because of the chemical reaction during processing. For example, slow filling may cause premature gelling, which results in short shots, whereas fast filling may induce turbulent flow, creating internal porosity. Moreover, the low viscosity of the material tends to cause flash that requires trimming. Another disadvantage of RIM is that the reaction with isocyanate requires special environmental precaution due to health issues. Finally, like many other thermosetting materials, the recycling of RIM parts is not as easy as that of thermoplastics. Polyurethane materials (rigid, foamed, or elastomeric) have traditionally been synonymous with RIM as they and urea urethanes account for more than 95% of RIM production.

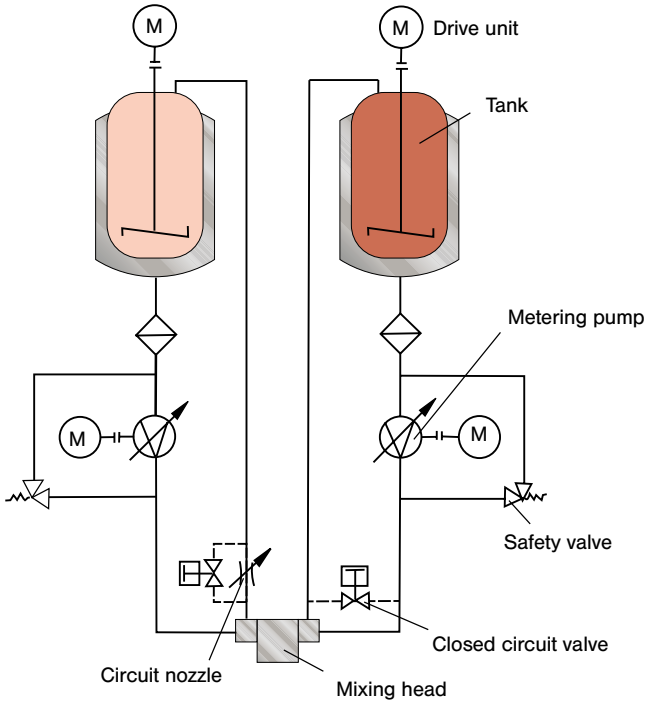

Figure 6.23 Schematic diagram of a high pressure polyurethane injection system.

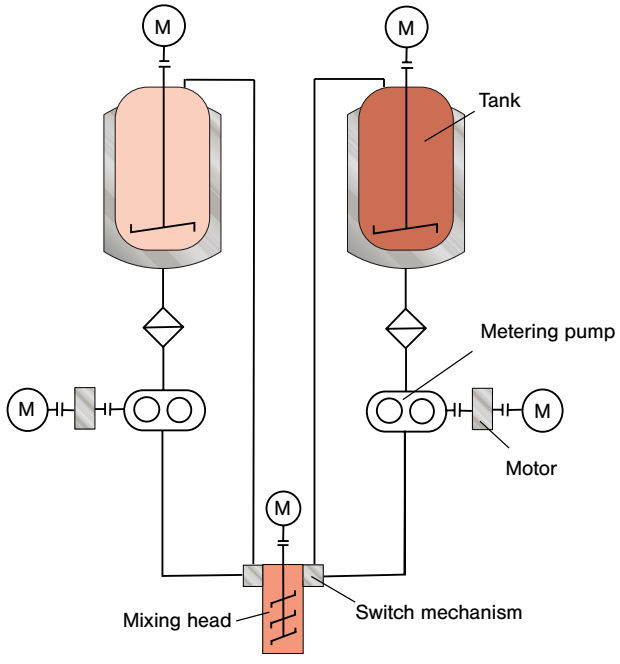

Figure 6.24 Schematic diagram of a low pressure polyurethane injection system

7 Additive Manufacturing

Dominik Rietzel[1], *Martin Friedrich*[1], *and Tim A. Osswald*

When we think of the history of additive manufacturing (AM), also known as 3D printing, at first glance it seems to be a recent development and some suggest the technology is a main accelerator for the new industrial revolution in the context of digital production. However, the idea is more than 100 years old, and the first patent application, for a method for producing topographical contour maps by cutting wax sheets and stacking them, was granted to J.E. Blanther in 1892 [1]. This concept was applied to a manufacturing process in 1984, when the patent for stereolithography was filed [2]. Unfortunately, the filing of those patents did not lead to a breakthrough of the technologies in the beginning as computational power was poor and the part properties were just good enough for geometrical prototyping applications. Today, over 30 years later, what was first called rapid prototyping has been renamed *additive manufacturing* as it expresses the original idea of the technology and not the initial use. Numerous technologies exist that are used to automatically manufacture near net-shape parts directly from CAD data. After the main patents ran out in the field of Fused Deposition Modeling (FDM) and stereolithography (SLA) the biggest hype started for the use of additive manufacturing at home and on desktops. This led to new ideas and innovations from startups but also to huge investments of global companies in various areas ranging from software, machines, and materials to applications.

Traditionally, in additive manufacturing, the three-dimensional parts are built layer by layer, which is why these processes are often referred to as *layered manufacturing* – basically a 2.5-D method. With new technologies, the idea of building a part voxel by voxel, defining infinitesimal volumes with different properties, is gaining more importance, as new file formats, such as 3MF[2], and today's computational capabilities are able to process more than just one simple layer at a time. Thus, recent trends are moving additive manufacturing towards true three-dimensional freeform manufacturing. In addition to usage of the various additive manufacturing processes to produce prototypes or actual products, it is sometimes also used in an in-

1) BMW Group, Munich, Germany

2) 3MF stands for 3D Manufacturing Format which was developed and published by the 3MF Consortium formed by companies such as 3D Systems, Autodesk, General Electric, Hewlett Packard, Materialise, Microsoft, Siemens, Stratasys, and Ultimaker, to name a few.

direct way, such as for the production of molds or tools, a field referred to as *additive tooling*.

Table 7.1 presents a summary of additive manufacturing techniques broken down into the suggested ISO/ASTM additive manufacturing categories and names [3]. The table presents alternative names, often coined as tradenames by the original inventors and companies that commercialized the different techniques. Additive processes can be classified by the initial state of the material, which can be gaseous, liquid, or solid. The various categories are presented in more detail in the subsequent sections.

The general additive manufacturing technique is schematically presented in Figure 7.1. The process begins by transforming a CAD model into a surface-based file format such as the STL[3] format, which is still a standard today. The STL format transforms a complex CAD surface representation to a surface approximated with triangles, after which it is more easily divided into two dimensional slices, which are then physically reproduced using the AM process. Depending on which technology is used, the slices can have a height of a few nanometers to some millimeters, which influences the stair-stepping effect on the generated parts. As mentioned, today there are attempts to define small volumes, so called voxels, instead of layers, which leads to a need for new file formats. These file formats provide the possibility to define different physical properties, such as color, stiffness, density, or conductivity, directly in the transfer file format, instead of generating these subsequently on the machine. These formats might also be helpful and needed for those new technologies that process in volumes instead of layers.

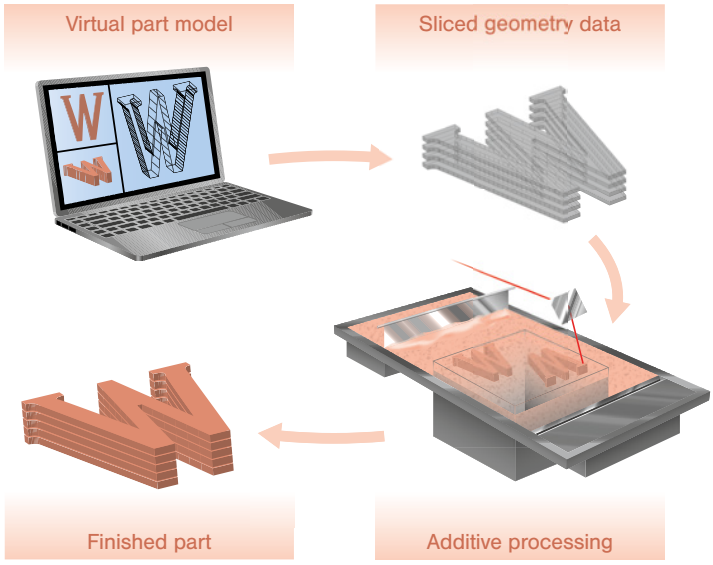

Figure 7.1 Schematic workflow of a typical additive manufacturing technique

[3] The name STL is derived from stereolithography, originally developed by 3D Systems to represent complex CAD geometries. However, because of its surface representation using triangles, STL is often assumed to be acronym for Standard Transformation Language.

Table 7.1 Additive manufacturing techniques

ASTM AM Name	Alternate Name	Date of Invention	Patent or Publication
Vat Photopolymerization (VPP)	Stereolithography (SLA or SL)	1984	US4575330 [2]
	Solid Ground Curing (SGC)	1986	US4961154 [4]
	Continuous Liquid Interface Production (CLIP)	2015	WO2016140891 [5, 6]
Powder Bed Fusion (PBF)	Selective Laser Sintering (SLS or LS)	1986	US4938816 [7]
	Multi Jet Fusion		HP Brochure [8]
	Selective Heat Sintering	2008	US9421715 [9]
Material Extrusion	Fused Deposition Modeling (FDM) Fused Filament Fabrication (FFF)	1989	US5121329 [10]
Sheet Material Lamination (SML)	Laminated Object Manufacturing (LOM)	1996	US5730817 [11]
Binder Jetting	Selective Binding or 3D Printing	1989	US5204055 [12, 13]
Material Jetting (MJ)	Wax Jetting	1989	US5136515 [14]
	Polymer Jetting or Freeforming	2013	EP2266782A1 [15]

7.1 Vat Polymerization Processes

As the name implies, vat polymerization additive manufacturing processes make use of a vat or container filled with a liquid or unpolymerized photopolymer. The part is built up inside this container by curing or polymerizing the resin layer by layer using a defined light source such as ultraviolet light. Various vat polymerization processes are discussed below.

7.1.1 Stereolithography (SLA)

SLA is a process that uses a thermosetting resin that cures by UV radiation

Stereolithography (SLA), schematically depicted in Figure 7.2, is a technique where an ultraviolet laser beam is used to cure a liquid photopolymer layer by layer. The method uses a platform that sits in a vat containing a liquid epoxy resin or an acrylate resin. During the build process, the platform sits just below the surface of the resin and an elevator is used to incrementally lower the platform after each layer of the photo-sensitive polymer has been exposed to the ultraviolet light by the highly focused laser beam. The laser scans the predefined area according to the slice information and cures the resin in a defined penetration depth. Subsequently, the plat-

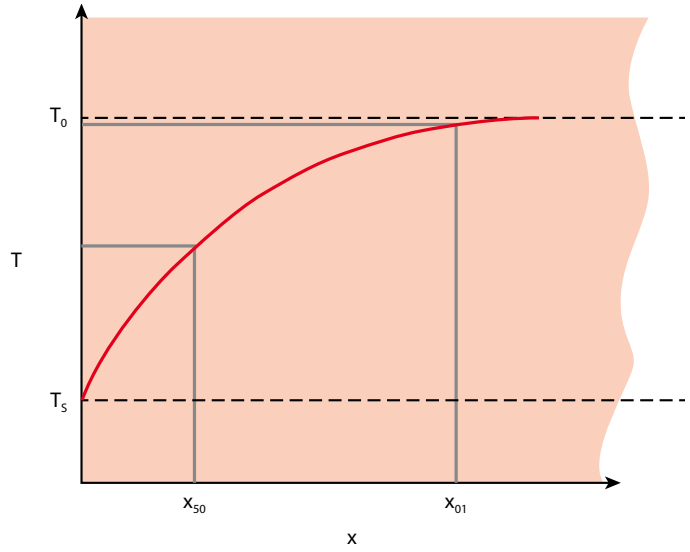

Figure 9.23 Schematic of a semi-infinite cooling body. Denoted are depths at which 50 % and 1 % of the temperature difference is felt

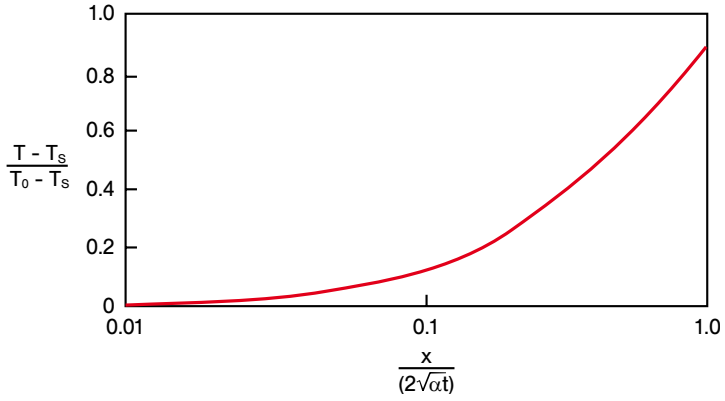

Figure 9.24 Dimensionless temperature as a function of dimensionless time and thickness

Table 9.6 Penetration Thickness and Characteristic Times in Heating and Cooling of Polymers

L	$T = L_2/\alpha$
100 μm	0.025 s
1 mm	2.5 s
2 mm	10 s
10 mm	250 s

For example, Figure 9.23 presents two depths, one where 1 % and another where 50 % of the temperature differential is felt. The 1 % temperature differential is defined by

$$T = T_0 + 0.01\left(T_S - T_0\right) \tag{9.112}$$

or

$$0.99 = \operatorname{erf}\left(\frac{x_{01}}{2\sqrt{\alpha t}}\right) \tag{9.113}$$

which can be used to solve for the given time that leads to a 1 % temperature change for a given depth x_{01}:

$$t_{01} = \frac{{x_{01}}^2}{13.25\alpha} \tag{9.114}$$

The same analysis can be carried out for a 50 % thermal penetration time:

$$t_{50} = \frac{{x_{50}}^2}{0.92\alpha} \tag{9.115}$$

Hence, the time when most of the temperature difference is felt by a part of a given thickness is of the order

$$t = \frac{L^2}{\alpha} \tag{9.116}$$

which can be used as a characteristic time for a thermal event that takes place through diffusion. Because polymers have a thermal diffusivity of about $10^{-7}\,\mathrm{m^2/s}$, we can easily compute the characteristic times for heating or cooling as a function of part thickness, 2 L. Some characteristic times are presented as a function of thickness in Table 9.6.

With a characteristic time for heat conduction we can now define a dimensionless time using

$$Fo = \frac{L^2}{\alpha t} \tag{9.117}$$

The Fourier number is the ratio of the time it takes for a part to reach thermal equilibrium by diffusion to a characteristic process time

which is the well known Fourier number.

Cooling and heating of a finite thickness plate. A more accurate solution of the above problem is to determine the cooling process of the actual part, hence, one of finite thickness 2 L. For the heating process of a finite thickness plate we can solve Eq. (9.109) to give

$$\frac{T - T_S}{T_S - T_0} = 1 - \frac{4}{\pi}\sum_{n=1}^{\infty}\frac{(-1)^{n-1}}{2n-1}\cos\left[\frac{(2n-1)\pi x}{L}\right]\exp\left(-\left[\frac{(2n-1)\pi^2}{2}Fo\right]\right) \tag{9.118}$$

Figure 9.25 presents the temperature history at the center of the plate and Figure 9.26 shows a comparison between the prediction and a measured temperature development in an 8 mm thick PMMA plate. As can be seen, the model does a good job of approximating reality.

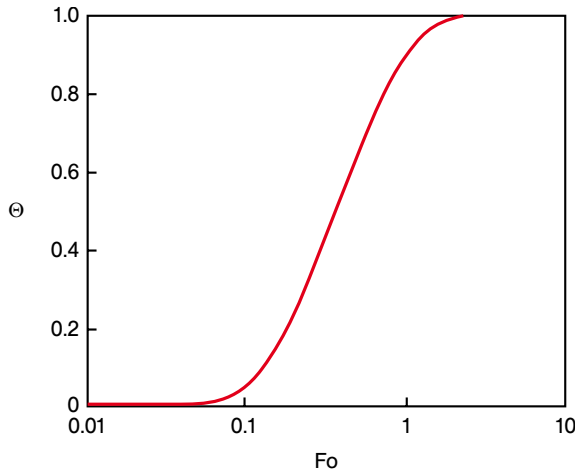

Figure 9.25 Center-line temperature history during heating of a finite thickness plate. Note that cooling is represented by the same curve using $1-\Theta$ as the dimensionless temperature

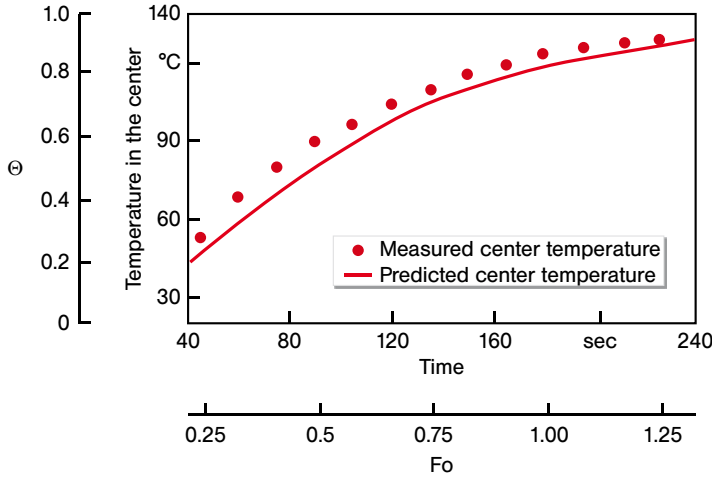

Figure 9.26 Experimental and computed center-line temperature history during heating of an 8 mm thick PMMA plate. The initial temperature T_0 = 20 °C and the heater temperature T_S = 140 °C [7]

Cooling and heating of a finite thickness plate using convection. As mentioned earlier, cooling with air or water is very common in polymer processing. For example, the

cooling of a film during film blowing is controlled by air blown from a ring located near the die exit. In addition, many extrusion operations extrude into a bath of running chilled water. Here, the controlling parameter is the heat transfer coefficient h, or in dimensionless form the Biot number, Bi, given by

$$B_i = \frac{hL}{k} \tag{9.119}$$

An approximate solution for the convective cooling of a plate of finite thickness is given by Agassant et al. [15]

$$\frac{T - T_f}{T_0 - T_f} \approx e^{(-BiF_o)} \cos\left(\sqrt{Bi}\,\frac{x}{L}\right) \tag{9.120}$$

The center-line temperature for plates of finite thickness is given in Figure 9.26 and a comparison between the prediction and experiments for an 8 mm thick PMMA plate cooled with a heat transfer coefficient, h, of 33 W/m^2/K is given in Figure 9.27. As can be seen, theory and experiment are in relatively good agreement.

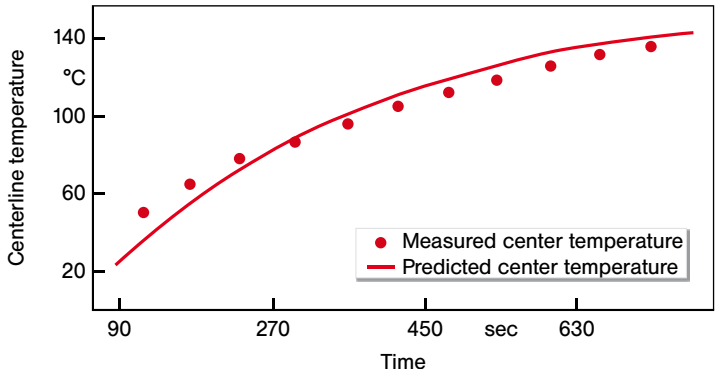

Figure 9.27 Center-line temperature history of an 8 mm thick PMMA plate during convective heating inside an oven set at 155 °C. The initial temperature was 20 °C. The predictions correspond to a Biot number, Bi = 1.3 or a corresponding heat transfer coefficient, h = 33 W/m^2/K [7]

■ 9.5 Mechanics of Particulate Solids

Particulate solids, powders, or granulated materials are encountered everywhere in polymer processing. The size of the particles can be as large as several millimeters, corresponding to plastic pellets, to a few micrometers in size for fine powders. Understanding the movement and compaction of particulate solids is not only important when dealing with processes such as rotational molding and selective laser

Index